Article

Additions to the taxonomy of the armadillo ants (Hymenoptera, Formicidae, *Tatuidris*)

DAVID A. DONOSO

Graduate Program in Ecology and Evolutionary Biology, Department of Zoology, University of Oklahoma, Norman, OK 73019, USA. Museo de Zoología QCAZ, Escuela de Ciencias Biológicas, Pontificia Universidad Católica del Ecuador, Aptdo 17-01-2184, Quito, Ecuador.
E-mail: david.donosov@gmail.com

Abstract

The taxonomy of the rare ant genus *Tatuidris* is revised by studying morphological variability among 118 specimens from 52 collection events in 11 countries, and sequences of Cytochrome Oxidase 1 (CO1 'DNA barcodes') of 28 specimens from 13 localities in 6 countries. *Tatuidris* are cryptic ants that inhabit the leaf litter of Neotropical forests from Mexico to French Guiana, central Brazil, and Peru. Based on the extent of the morphological variability encountered throughout this broad geographic range, *T. kapasi* is relegated to junior synonymy under *T. tatusia*. Analysis of barcodes indicated a pattern of genetic isolation by distance, suggesting the presence of a single species undergoing allopatric differentiation. The genus *Tatuidris*, thus, remains monotypic. Male and female reproductive castes are described for the first time.

Introduction

The ant genus *Tatuidris* comprises cryptic ants that inhabit the leaf litter in the Neotropics (Brown and Kempf 1968). Workers of *Tatuidris* present a distinctive morphology (Figure 1), consisting of a shield-like head with a broad vertex, ventrally-turned heavy mandibles which do not overlap at full closure, deep antennal scrobes with eyes at or close to their apex, compact and fused mesosoma, 7-segmented antenna, first gastral segment ventrally directed, and unique among ants—an antenna socket apparatus sitting upside down on the roof of the expanded frontal lobe (first described in Keller 2011, see his figures 12B and 12C). These characteristics, combined with a thick integument and a generally rounded habitus, are reminiscent of armadillos. Both "tatuidris" and "tatusia" mean "armadillo" (Brown and Kempf 1968) which is the common name for this genus (Lacau *et al.* 2012).

Taxonomy summary

Brown and Kempf (1968) described the genus *Tatuidris* to contain the newly described species *tatusia*. Due to morphological similarities, they included *T. tatusia* in what was then a myrmicine tribe, the Agroecomyrmecini. The tribe also includes two fossil genera, *Agroecomyrmex* Wheeler from the Baltic amber [44.1 Million years (Myr) ago] and *Eulithomyrmex* Carpenter from the Miocene Florissant Shale of Colorado in North America (34 Myr ago; Carpenter 1930, 1935; Moreau and Bell 2011). Since the original description, the systematic status of the tribe has been the focus of intense debate. Due to similarities in the habitus, Brown and Kempf (1968) linked *Tatuidris* to the Dacetini genus *Glamyromyrmex* (currently a junior synonym of *Strumigenys*) and *Phalacromyrmex*. However they concluded: "analysis of these similarities indicates […] that they are mostly convergent and not based on close phylogenetic relationship" (Brown and Kempf 1968:183). Further work explored the similarities of *Tatuidris* with *Ishakidris* (Bolton 1984) and *Pilotrochus* (Brown 1977). While these taxa share some characteristics, including an expanded head vertex, deep antennal scrobes and a compact mesosoma, the similarities were again deemed convergent (Bolton 1984).

Bolton (2003) was the first to suggest the taxonomic instability of *Tatuidris* within Myrmicinae and raised the genus to the level of a new subfamily, the Agroecomyrmecinae. This assessment was based on the following diagnostic characters: 1) large mandibles with mandibular masticatory margins that oppose at full closure but do

not overlap, 2) eyes at extreme posterior apex of deep antennal scrobes, 3) clypeus very broadly triangular, broadly inserted between the frontal lobes, 4) antennal sockets and frontal lobes strongly migrated laterally, far apart and close to lateral margins of the head, 5) mesotibia and metatibia with pectinate spurs, 6) short and compact mesosoma, 7) a sessile petiole, in posterior view the tergite and sternite not equally convex, 8) an abdominal segment III (postpetiole) without tergosternal fusion, segment large and very broadly articulated to segment IV, 9) a helcium in frontal view with the sternite bulging ventrally and overlapped by the tergite, 10) an abdominal segment IV with a complete tergosternal fusion [note: this character was described incorrectly by Bolton (l.c.); in *Tatuidris* the tergosternal suture of the abdominal segment IV is strong but not fused], 11) abdominal segment IV with a stridulitrum on the pretergite, and 12) the sternite of abdominal segment IV is reduced, the tergite is much larger than the sternite and strongly vaulted.
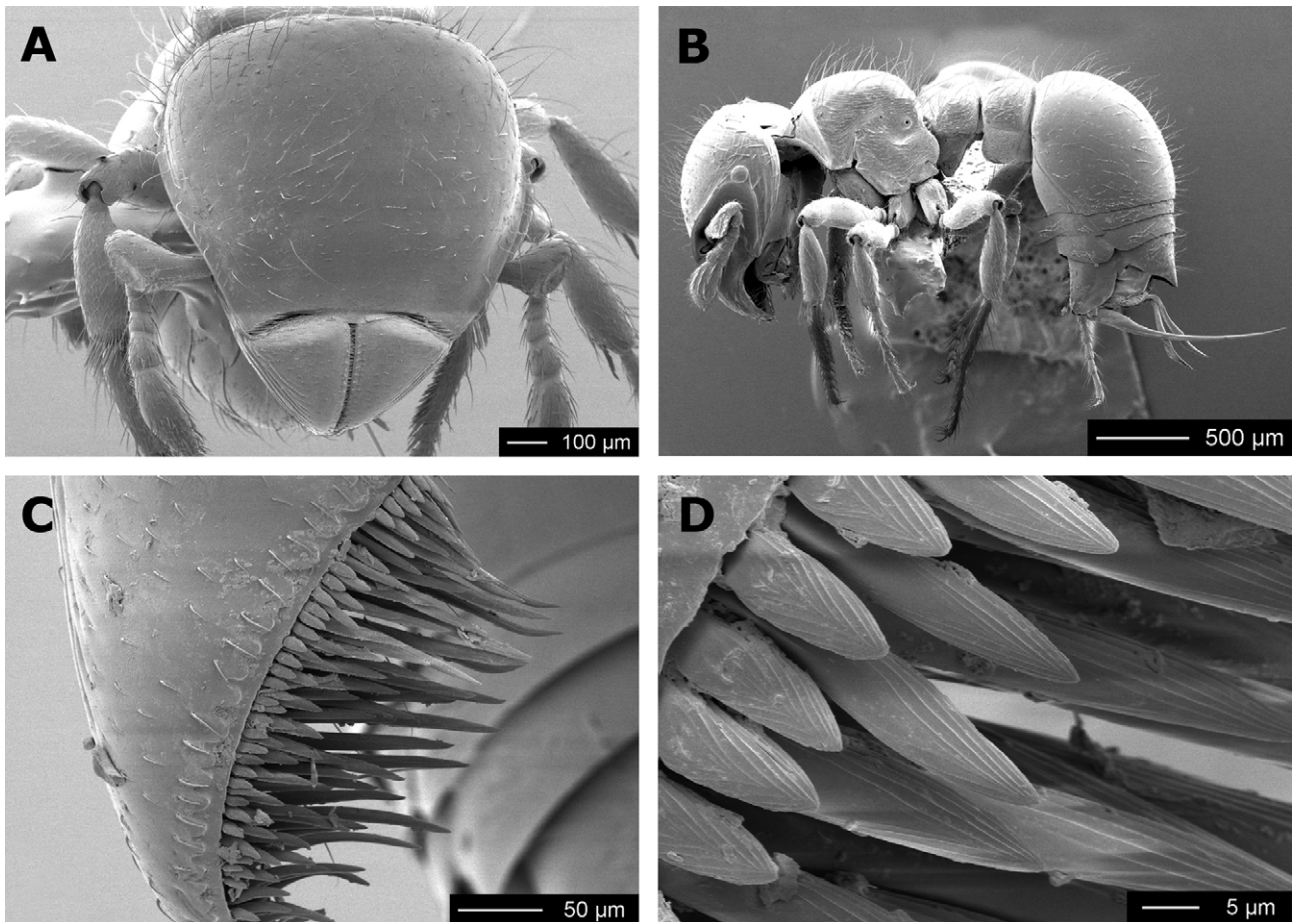

FIGURE 1. SEM images of *Tatuidris tatusia* external morphology. A) Head in (partial) full-face view; B) lateral view of the body; C) mandibular setae; D) close-up of mandible setae.

The subfamily rank of the armadillo ants was re-assessed by Baroni Urbani and de Andrade (2007) in their last systematic assessment of the dacetines. They analyzed a relatively large morphological dataset (54 characters from 24 terminal taxa) that included former dacetines, basicerotines, phalacromyrmecines and *Tatuidris* as well as other non-Myrmicinae taxa such as the Australian genus *Myrmecia* and the Neotropical genus *Pseudomyrmex*. This work was the first attempt to include the ant genus *Tatuidris* as a terminal taxon in a morphological cladistic analysis. In their study, Baroni Urbani and de Andrade (2007:78) identified six morphological synapomorphies shared between *Tatuidris* and the dacetines, justifying the inclusion of the genus within Myrmicinae. These characters included 1) mandibles at rest opposing at least in part, instead of crossing, 2) a mandibular-torular index < 130, 3) reduction of maxillary palps from 2-jointed to 1-jointed, 4) reduced male mandibles, 5) presence of a two-segmented antennal club, and 6) a reduced number of antennal joints. In addition, two autapomorphies (a differently shaped petiolar tergum and sternum, and the eyes at or close to the apex of the antennal scrobe) separated *Tatuidris* from all other extant ant genera included in their study (Baroni Urbani and de Andrade 2007).

Unlike phylogenetic studies based on morphological traits, molecular analyses of the internal phylogeny of the ants have given strong evidence that the armadillo ants are neither closely related to nor nested within the Myrmicinae. Brady *et al.* (2006), Moreau *et al.* (2006) and Rabeling *et al.* (2008) reconstructed phylogenetic trees with the agroecomyrmecines inside the 'poneroid' group of subfamilies, close to the Paraponerinae, and gave support for the exclusion of the genus from the Myrmicinae, a subfamily located inside the 'formicoid' clade (Ward 2009). Given the early appearance of the Agroecomyrmecinae in the geologic record, the similarities of armadillo ants to Myrmicinae were hypothesized to represent convergence and/or retention of plesiomorphic forms (Ward 2011).

Recently, Keller (2011) challenged the phylogenetic relationships of the poneromorph subfamilies (including *Tatuidris*). This study included a large set of taxa and morphological characters, several of them coded and illustrated for the first time. Interestingly, *Tatuidris* was again grouped close to Myrmicinae, however, Myrmicinae also nested inside the poneromorphs (Keller 2011).

Justification for a taxonomic revision

Since its description more than 40 years ago, no modern systematic account of *Tatuidris* has been done. Over this time, many *Tatuidris* specimens have accumulated in regional ant collections and country inventory lists (Bolton 1984, Rojas 1996, Vasconcelos and Vilhena 2003, Fernández 2002, Vieira 2005) and these have been assigned to potential morphospecies (Longino *et al.* 2002) and species (Lacau *et al.* 2012). In the present work, I review *Tatuidris* specimens from localities throughout the Neotropics, I describe morphological and genetic variability encountered across the range, and I described for the first time the male and female reproductive castes of the genus.

Materials and methods

Tatuidris is a rare but broadly distributed genus. The primary sources of specimens in this study are museum collections and specimen loans. In cases when travel or loans were not feasible, specimens were analyzed from photographs. However, efforts were made to review type material deposited at the MCZ. In total, this study comprises 118 specimens from 52 collection events (the proportion of specimens to collection events was 2.26 and the average number of collection events per country was 4.3). Several specimens included in this this study have been imaged and are available on AntWeb (www.antweb.org), Ants of Costa Rica (www.evergreen.edu/ ants/ AntsofCostaRica.html) or at the Museum of Comparative Zoology at Harvard (Gary Alpert). Specimens studied come from the following ant collections:

CASC	California Academy of Sciences, San Francisco, USA.
CPDC	Centro de Pesquisa do Cacau, Ilheus, Brazil.
INBC	Instituto National de Biodiversidad, San José, Costa Rica.
INPA	Instituto de Pesquisas da Amazônia, Manaus, Brazil.
IEXM	Instituto de Ecología AC de Xalapa, Xalapa, Mexico.
JTLC	John T. Longino Collection, Salt Lake City, USA.
MCZC	Museum of Comparative Zoology, Cambridge, USA.
MEKC	Michael E. Kaspari Collection, Norman, USA.
MUSM	Museo de Historia Natural "Javier Prado", Lima, Perú.
MZSP	Museu de Zoologia da Universidade de São Paulo, São Paulo, Brazil.
QCAZ	Museo de Zoología de la Universidad Católica, Quito, Ecuador.
WEMC	William and Emma MacKay Collection, El Paso, USA.

Observations were made at 66x on a Zeiss Stemi SV11 dissecting microscope and at 90x on an Olympus SZX12 dissecting microscope. Measurements were taken to the nearest 0.01mm. Male morphology nomenclature follows Yoshimura and Fisher (2007, 2009). Wing venation follows Serna *et al.* (2011). Measurements and indices are defined as follows:
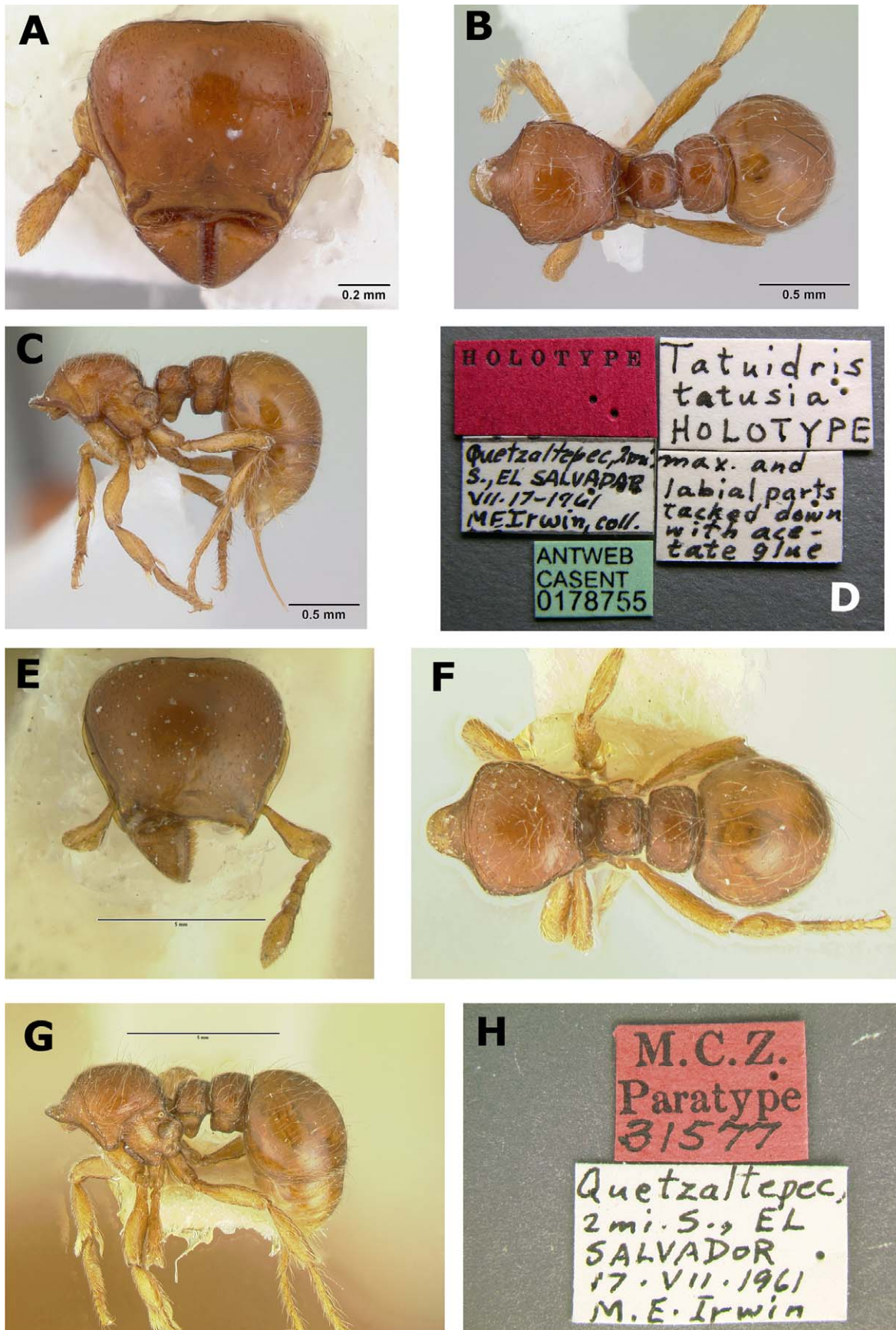
FIGURE 2. *Tatuidris tatusia* type series, showing pilosity pattern A. A–D) Full face view, lateral view, dorsal view, and label of *T. tatusia* Holotype; E–G) Full face view, lateral view, dorsal view, and label of *T. tatusia* Paratype (MCZ collection Type locality: El Salvador [Brown and Kempf 1968]). Images A–D courtesy of antweb.org.

AScL. Antennal scrobe length, from the anterior angle to its apex, near the eye.

AScW. Width of antenna scrobe at its widest.

EL. Length of compound eye, at its longest.

FFS. Length of the first funicular segment (male and gyne only).

FL. Fore femur length, excluding the condyle.

FW. Fore femur width, at its widest.

HL. Head length, measured with head in full-face view, from the anterior median clypeal border (not including the clypeal apron) to the median posterior border.

HW. Head width, measured with head in full-face view. The measure is taken anteriorly to the eyes, where the antenna carina starts. In workers and gynes, HW does not include the eyes. In male, HW includes the eyes.

IAD. Inter-antenna distance. This measure is taken in full-face view and corresponds to the distance between the internal edges of the antenna fossae. In most workers (and gyne), the antenna fossa is visible through the cuticle as a blister or translucent cavity.

PL. Petiole length, measured along line parallel to tergosternal suture, from anterior-most to posterior-most visible portions of tergite.

PW. Petiole width, in dorsal view.

PpL. Postpetiole length, measured along line parallel to tergosternal suture, from anterior-most to posterior-most visible portions of tergite.

PpW. Postpetiole width, in dorsal view.

PrW. Pronotum width, in dorsal view.

SL. Scape length. Because the antenna inserts upside-down, the antennal condyle can be easily seen in full-face view inside the antenna fossa (which appears like a blister). Scape length is taken from the center-point of this antenna fossa to the outer edge of the scape, including the cuticle ridge. This measurement includes the antenna condyle and condyle neck.

SW. Scape width, at its widest.

TiL. Hind tibia length.

TiW. Hind tibia width.

WbL. Weber's length, in lateral view, from the base of anterior slope of pronotum to the lower posteroventral angle of propodeum.

WingL. Forewing length (male and gyne only).

Indices

CI. Cephalic index (HW × 100/HL).

PPpI. PW × 100/PpW.

REL. Relative eye size (EL × 100/HL).

SI. Scape index (SL × 100/HW).

Morphometric analysis

Patterns of morphological variation were summarized with a Principal Component Analysis (PCA). The PCA was done on the correlation matrix of 14 morphological variables (AScL, AScW, EL, HL, HW, IAD, PL, PpL, PW, PpW, PrW, TiL, TiW, WbL) and 37 specimens (that included 4 different pilosity patterns) for which all variables were measured. The correlation matrix was chosen because it gives equal weights to all morphological variables without regard to their relative size. Principal components explaining more than 1% of the variation were retained. Principal component-1 (PC-1) was generally interpreted as summarizing the variation in size magnitude among specimens. Variation summarized by PC-2, PC-3 and PC-4 was interpreted as shape variability.

DNA Barcode Analysis

Sequences of the mitochondrial gene Cytochrome Oxidase 1 (CO1), DNA barcodes, for 28 specimens from 13 localities in 6 countries were obtained in collaboration with the Biodiversity Institute of Ontario and the Barcode of Life Database (BOLD, Ratnasingham & Hebert 2007). Samples used for molecular analysis came mostly from mounted specimens in museum collections, and sequences provided by ongoing projects, courtesy of John Longino (Project LLAMA) and Alex Smith. Usually, hind legs were removed from specimens and sent for analysis to

BOLD. DNA extraction, PCR, and sequencing reactions followed the procedures described in Hebert *et al.* 2003 and Fisher and Smith 2008. Only sequences greater than 500 bp were included in analyses. Collection data, sequences, and GenBank accession numbers are available in Table 1, and in the project 'TATU – Tatuidris of the Neotropics' publicly available at http://www.barcodinglife.org. An additional barcode sequence for *T. tatusia* (Moreau *et al.* 2006) and four outgroup ant taxa (i.e. *Paraponera clavata, Proceratium avium, Probolomyrmex* sp., and *Strumigenys coveri*) were extracted from Genbank. Recently, *Paraponera clavata* was recovered as the closest taxon to *Tatuidris* (Moreau *et al.* 2006, Ward 2011).

TABLE 1. Genbank accession numbers. Species, BOLD accession numbers, simple ID and country of origin are provided.

Species	Genbank	BOLD accession	Sample ID	Country
Tatuidris tatusia	HQ545899	ACGAD630-10	10COSTA-0629	Costa Rica, Guanacaste, Pailas
Tatuidris tatusia	HQ545900	ACGAD631-10	10COSTA-0630	Costa Rica, Guanacaste, Pailas
Tatuidris tatusia	JX827985	ASPAN476-11	4130219_JJ	Ecuador Zamora
Tatuidris tatusia	JN282603	ACGAE585-11	BIOUG00400-E04	Costa Rica, Guanacaste, Pailas
Tatuidris tatusia	HM434648	ASLAM227-10	CASENT0609802	Mexico Chiapas
Tatuidris tatusia	HM434649	ASLAM228-10	CASENT0610404	Guatemala Peten
Tatuidris tatusia	HM434653	ASLAM232-10	CASENT0610405	Guatemala Peten
Tatuidris tatusia	HM434650	ASLAM229-10	CASENT0610412	Guatemala Peten
Tatuidris tatusia	HM434654	ASLAM233-10	CASENT0610645	Guatemala Peten
Tatuidris tatusia	JN283742	ASLAM779-11	CASENT0615397	Honduras Comayagua
Tatuidris tatusia	JN283743	ASLAM781-11	CASENT0615399	Honduras Comayagua
Tatuidris tatusia	JN283744	ASLAM782-11	CASENT0615400	Honduras Comayagua
Tatuidris tatusia	JN283745	ASLAM783-11	CASENT0615401	Honduras Comayagua
Tatuidris tatusia	HM434652	ASLAM231-10	INB0003618364	Costa Rica Heredia
Tatuidris tatusia	HM434651	ASLAM230-10	INB0003654764	Costa Rica Heredia
Tatuidris tatusia	HM434647	ASLAM226-10	INB0003678143	Costa Rica Heredia
Tatuidris tatusia	JX827981	ASPAN487-11	LL4_P3_W1_GR	Ecuador Pichincha Toachi
Tatuidris tatusia	JX827982	ASPAN199-10	MEKOU012083	Ecuador Pichincha Toachi
Tatuidris tatusia	JF863787	ASPAN200-10	MEKOU012084	Ecuador Pichincha Toachi
Tatuidris tatusia	JX827986	ASPAN203-10	MEKOU012085b	Mexico Veracruz Tuxtlas
Tatuidris tatusia	JF863788	ASPAN210-10	MEKOU012092	Nicaragua Matagalpa
Tatuidris tatusia	JF863790	ASPAN220-10	MEKOU012093b	Ecuador Cotopaxi La Mana
Tatuidris tatusia	JF863789	ASPAN217-10	MEKOU012096	Mexico Veracruz Tuxtlas
Tatuidris tatusia	JF863791	ASPAN221-10	MEKOU012100	Mexico Tamaulipas
Tatuidris tatusia	JF863792	ASPAN222-10	MEKOU012101	Mexico Tamaulipas
Tatuidris tatusia	JX827984	ASPAN493-11	MGB_1179A	Nicaragua Matagalpa
Tatuidris tatusia	JX827983	ASPAN494-11	MGB_1179B	Nicaragua Matagalpa
Tatuidris tatusia	DQ353314.1		RA0399	Mexico Veracruz Tuxtlas
Paraponera clavata	AY233687.1			
Probolomyrmex sp.	DQ353287			
Strumigenys coveri	DQ176245.1			
Proceratium avium	EF610176.1			

To assess the discriminatory power of barcodes, I calculated sequence divergence using the Kimura 2 parameter distance model (K2P) and built a Neighbor Joining (NJ) tree using MEGA version 5.1 (Tamura *et al.* 2007). This procedure does not constitute a strict phylogenetic analysis of the barcode sequences. Support for tree branches was calculated using 999 bootstrap replicates.

Results

Genus *Tatuidris*

Tatuidris Brown and Kempf 1968:183. Type species: *Tatuidris tatusia* Brown and Kempf 1968:187, by monotypy.

Worker: HW = 0.56–1.10mm. Body short and compact. Color ferruginous to dark red. Integument thick and rigid. Body covered by hairs, which are variable in length and inclination. HEAD. Head shape pyriform, broadest behind. Maxillary palps one-jointed. Labial palps two-jointed. Labrum bilobed, broader than longer, capable of full reflexion over the buccal cavity. Mandibles opposing in most of their border (except in the tips of the masticatory margin). Masticatory margin with two blunt apical teeth overlapping at closure. Setae (mandibular brush) abundant, present on the ventral side of mandibles. Antenna 7-segmented. Antennal club two segmented, well developed. Scape clavate, gently downcurved at base. Torulus with hypertrophied dorsal lobe and strongly curved downwards. Antennal scrobe present. Antennal socket and antennal scrobe confluent. Antenna socket apparatus sitting upside down on the roof of the expanded frontal lobe. Eyes present, small (REL= 5.41–11.48), located at the posterior apex of antennal scrobe. MESOSOMA. Promesonotal suture fused. Metapleural gland orifice round. Metapleural gland opening visible. Metapleural gland bulla separated from annulus of propodeal spiracle by more than the diameter of the spiracle. Katepisternal oblique groove absent. Lower mesopleuron with longitudinal costulae. Propodeum unarmed. Propodeal spiracle, in profile, located at about mid-length of sclerite. PETIOLE and POSTPETIOLE. Petiole short and sessile. Petiolar ventral process large and rounded. Petiole dorso-ventrally fused. Petiole broadly attached to postpetiole (abdominal segment III). Postpetiolar tergum and sternum overlapping at junction. Postpetiole in dorsal view wider in posterior half. GASTER. Articulation between postpetiole and gastral segment 1 (abdominal segment IV) broad. Postpetiolar postsclerites not set in a concavity or depression. Pretergite of first gastral segment with neck-like constriction. Stridulitrum present on first gastral segment. Limbus (i.e. anterior transverse cuticular ridge of the first gastral segment) absent. Suture between first gastral tergite and sternite anteriorly rounded. First gastral tergosternal suture strong, but not fused. Base of the first gastral sternum in profile rounded. First gastral sternite length is reduced, such that tergite is much larger than the sternite and strongly vaulted. First gastral tergum and sternum smooth or with scattered puncta. Sting present. LEGS. Mid and hind tibial spurs present.

Gyne: HW = 1.28mm. Body short and compact, with exterior morphology and characters similar to workers. Body covered by hairs. Color yellow, paler than workers. Integument thick and rigid. HEAD. Head shape pyriform, broadest behind. Vertex straight, not concave. Labrum bilobed, broader than long, capable of full reflexion over the buccal cavity. Mandibles opposing in most of their border, except in the tips of the masticatory margin. Masticatory margin with two blunt apical teeth overlapping at closure. Mandibular setae present but less abundant than in workers. Antennal joints 7-segmented. Antennal club two segmented, well developed. Scape clavate, gently downcurved at base. Antennal scrobe present. Antennal socket and antennal scrobe confluent. Antenna socket apparatus sitting upside down on the roof of the expanded frontal lobe. Eyes present, EL = 0.20mm, eyes larger than in workers (REL = 22.63), located laterally at posterior border of antennal scrobes. Lateral ocelli and median ocellus present. WINGS. WingL=4.60mm, about 60% longer than total body length. Forewing well developed, with costal cell, basal cell (radial), sub-basal cell (cubital), no vein present between sub-marginal cell 1 and sub-marginal cell 2, R1 vein surrounding sub-marginal cell 3, discal cell 1 and discal cell 2 present, divided by cubital vein which extends a distance similar to the inferior edge of discal cell. Hindwing well developed, with Cu-a vein present. Basal cell completely surrounded by M-Cu and and rs-m+M veins. MESOSOMA. Promesonotal suture present, not fused. Scutellum broad. Anepisternum and katepisternum broad and shiny, not sculptured. Propodeum armed with a small posteriorly directed spine.

Propodeal spiracle in profile at about one-diameter from posterior edge. Metapleural gland present, metapleural spiracle big, longer than broader, within a dorsally directed fold. PETIOLE and POSTPETIOLE. Petiole broadly attached to postpetiole (abdominal segment III). Postpetiole in lateral view much shorter than gaster (abdominal segment IV). GASTER. Shiny. Vaulted. Constriction between postpetiole and gaster present. Abdominal sternum IX simple, triangular in shape, without spines or lobes. Sting present. LEGS. Mid and hind tibia with pectinate spurs present.

Male: HW = 0.88mm. Body compact, with exterior morphology (except head) similar to workers. Body covered by decumbent setae. Color dark. HEAD. Dorsum with scrabrous-strigate sculture. Lateral ocelli and median ocellus present. Antenna 12-segmented. Antennal sockets exposed, not covered by frontal carinae, at mid-length from the anterior border of clypeus and the head posterior vertex margin. Antennal scrobes absent. Antennal carinae absent. Scape very short, about 1.3 times as long as pedicel. First flagellar segment relatively short, about the same length as pedicel, slightly curved at base. Antennal club absent, but apical segment is at least 2 times longer than preceding segment. Mandibles reduced, falcate, without differentiated masticatory and basal margins. Mandible edentate, with no visible apical tooth. Clypeus broad, with straight anterior margin. Clypeus does not extend to space between eyes. EL = 0.32mm, eyes larger than in workers (REL = 48.44) located at mid-length at lateral margin. WINGS. WingL = 3.6mm, about 50% longer than total body length. Venation and cell composition of both fore- and hind-wings similar to that of gyne. MESOSOMA. Oblique mesopleural furrow close to but not reaching pronotum. Mesonotum notauli absent. Mesoscutum and mesoscutellum mostly shiny, with small foveae. Pronotum with rugae. PETIOLE and POSTPETIOLE. Constriction between petiole and postpetiole (abdominal segment III)present. Petiole and postpetiole similar in shape to worker petiole and postpetiole. Petiole broadly attached to postpetiole. Postpetiole, in lateral view, much shorter than gaster (abdominal segment IV). GASTER. Shiny. Vaulted. Constriction between postpetiole and gaster present. Abdominal sternum IX simple, triangular in shape, without spines or lobes. LEGS. Hind tibia with 1 pectinate spur.
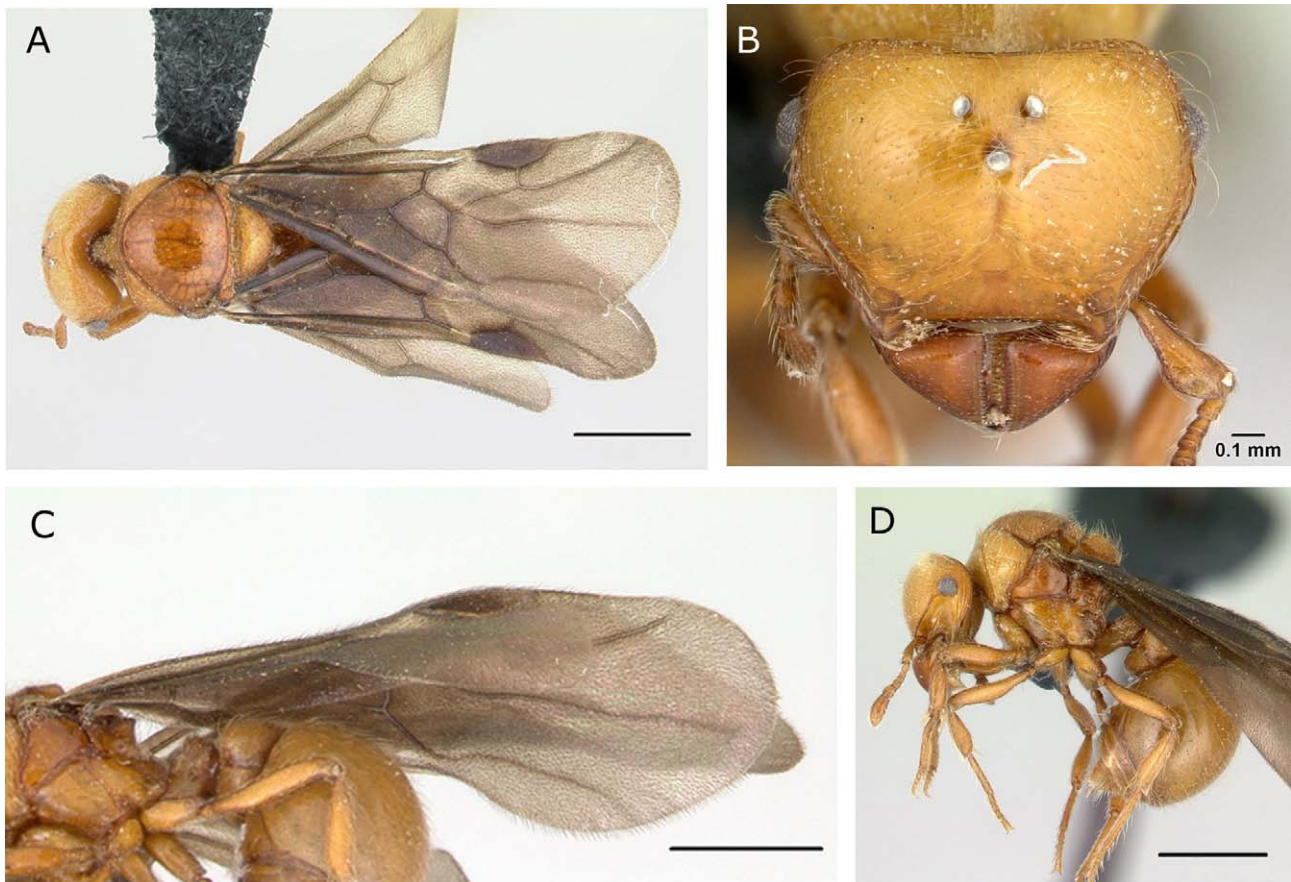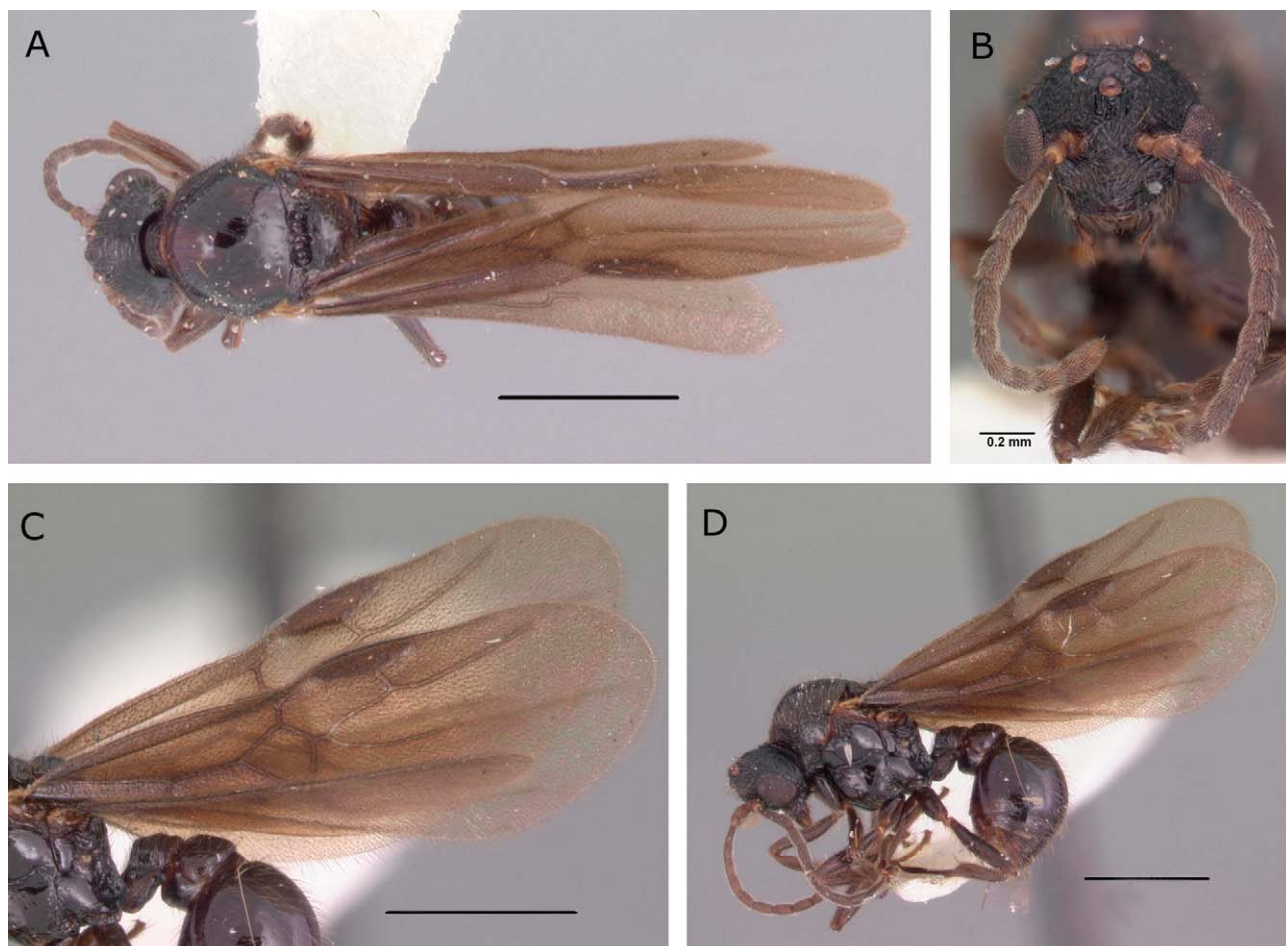

FIGURE 3. Images of *Tatuidris tatusia* gyne from Otongachi, Ecuador. Specimen CASENT 0178881. A) Dorsal view; B) Head in full face view; C) Detail of the wings; D) Lateral view of the body. All images courtesy of antweb.org.

Tatuidris tatusia Brown and Kempf 1968

Tatuidris tatusia Brown and Kempf 1968:187, their figures 1–4. Holotype and Paratype workers: El Salvador, La Libertad, 2 mi
S. Quetzaltepec ,VII-17-1961 (M.E. Irwin leg.) [holotype, UCDC] (image examined) [paratype, MCZC] (examined).
Tatuidris kapasi Lacau and Groc, *in* Lacau *et al*. 2012:2, their figures 1–6. Holotype worker: Guyane Francaise, Montagne de
Kaw, 04∘ 38.21′ N; 052∘ 17.36′ W, Alt. 260 m., ix.2008 (S. Groc, A. Dejean, and B. Corbara leg) [CPDC] (image
examined). *n. syn.*

Worker, male and gyne diagnosis: With same characters as in the genus description (Figures 1–4).

FIGURE 4. Images of *Tatuidris tatusia* male from Chiriqui, Panama. Specimen CASENT 0102681. A) Dorsal view; B) Head
in full face view; C) Detail of the wings; D) Lateral view of the body. All images courtesy of antweb.org.

Pilosity variability. Currently, four striking pilosity patterns are known to occur within *Tatuidris* collections
(Figure 5). Pilosity pattern A (Figure 6) consists of a mix of both long flexuous and short appressed setae. This is
the most common pilosity pattern and the one that most resembles the type specimens from El Salvador and the
gyne from Otongachi, Ecuador. Pilosity pattern B (Figure 7) is characterized by very short, fully appressed, and
regular spaced setae arrayed homogeneously and equidistantly on the head, mesosoma, petiole, postpetiole and
gaster. Pilosity pattern C (Figure 8) is characterized by dense lanose-looking setae. Pilosity pattern D (Figure 9)
consists of short and uniform decumbent (strongly inclined but not fully appressed) setae scattered throughout the
body.

DNA Barcodes. In total, 28 sequences (20 of them with full, 658bp, length) of the barcode gene were recovered
from BOLD and included in the analyses (Table 1). Among these sequences, 120 out of the 658 basepairs (18.23%)
were variable. In general, specimens (excluding colony duplicates) presented very high levels of intraspecific
pairwise differences (average = 5.36%, min = 0%, max=15.08%). The upper values of intraspecific pairwise
differences encountered here are well above the 2% usually recovered for species differences in DNA barcode

literature in general (Ratnasingham and Hebert 2007), and above the percentages of average intraspecific variability reported previously for ants (e.g. between the 1.67% and 6.37% encountered for *Anochetus* and *Odontomachus* in Madagascar by Fisher and Smith 2008; see also Smith and Fisher 2009, Jansen *et al.* 2009). Pilosity patterns present among individuals (excluding pilosity pattern "C" for which no sequence was available) were not in similar clusters as depicted on the NJ tree (Figure 10). Instead, four different clusters (groups) with strong geographic structure were observed: G1, Mexico+Honduras+Guatemala; G2, Costa Rica+Nicaragua; G3, Ecuador (West of Andes); and G4, Ecuador (East of Andes/Amazon Basin) (Figure 10). Furthermore, across this geographic range, pairwise barcode divergence among specimens was significantly related to distance (R^2=0.37, p<0.01, Figure 11).

Morph A
long flexuous + short setae
T. tatusia type

Morph B.
Very short setae

Morph C.
Abundant, lanose setae

Morph D
Regular spaced, short setae
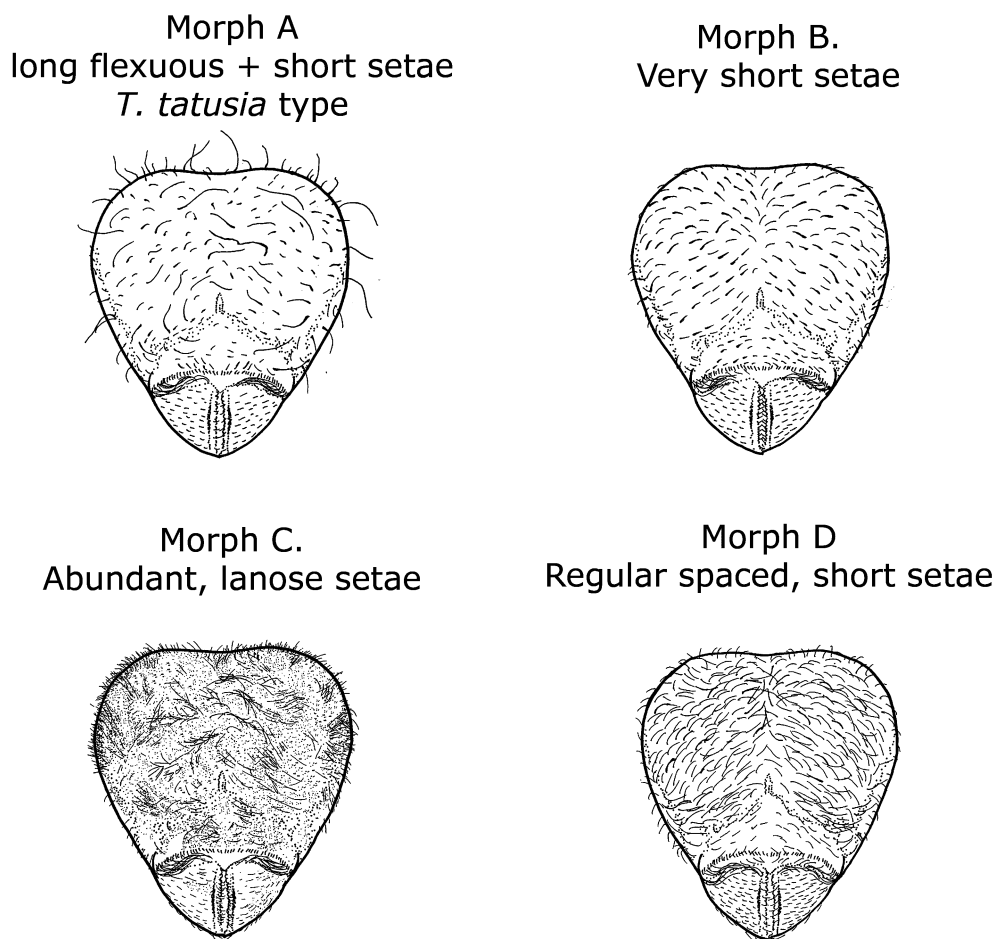
FIGURE 5. Visual representation of *Tatuidris* pilosity patterns. Images courtesy of Natalie Clay.

Size. Specimens of *T. tatusia* are small (average WbL = 0.62mm), but specimens can vary greatly in size, with larger specimens being twice as large as the smaller ones (min WbL = 0.45 mm, max WbL = 0.90 mm). Size variability within trap catches (possibly same colonies) may be considerable. For example, workers from one collection catch in Nicaragua (collection series MGB#1179) varied 30% in size (WbL from 0.65 to 0.85 mm). It is still unclear whether intra-colony size variation is due to the presence of morphological worker castes (e.g. minor and major castes) or continuous size variability. The PCA analysis revealed that most variability among specimens is related to size (proportion of variance explained by PC-1 = 0.915), with PC-2, PC-3 and PC-4 (e.g. shape) explaining little (0.033, 0.021 and 0.011, respectively) of total variation (Table 2). Eye length loaded positively and contrasted against all other variables, in PC2. Tibia length and tibia width loaded negatively and contrasted against most other variables, in PC3. Size variability summarized in this analysis was not related to pilosity patterns (Figure 12). In general no PC correlated with pilosity patterns. Hand drawings courtesy of Natalie Clay (Figure 12).

TABLE 2. First four PCA coefficients for morphological variables retained in this study. PC eigenvalues (% of variance explained) are also given.

Trait	PC1	PC2	PC3	PC4
AScL	0.2737	−0.0619	0.0329	0.2525
AScW	0.2730	−0.1618	−0.0559	0.1040
EL	0.2135	0.9362	−0.1003	−0.0722
HL	0.2761	−0.0490	0.0880	0.2140
HW	0.2780	−0.0043	0.0557	−0.0271
IAD	0.2749	−0.1594	0.0246	0.1754
PL	0.2679	−0.1677	0.1582	−0.4504
PpL	0.2643	0.0462	0.4339	−0.3384
PW	0.2739	−0.0537	0.1803	−0.1468
PpW	0.2758	0.0473	0.0436	0.1971
PrW	0.2767	0.0585	−0.0261	0.0450
TiL	0.2440	−0.1402	−0.8193	−0.4051
TiW	0.2672	−0.0193	−0.2126	0.5268
WbL	0.2752	−0.0823	0.0967	−0.1464
Eigenvalue	0.9154	0.0334	0.0211	0.0112

Sculpture. The strength and depth of all sculpture patterns is accentuated in larger sizes. Collections from Nicaragua also tend to present more accentuated sculpture patterns. The head dorsum is usually smooth and shining, except for the area below eyes, which presents longitudinal carinae. The head vertex is covered with transverse carinulae. The lateral surface of the mandible is smooth and shining except for longitudinal superficial striae on the side that vary in depth. The antennal scape is shagreened and superficially areolate. The surface of the ventrolateral part of the pronotum varies strongly across specimens, from smooth and shining to strongly striate, or carinulate. The dorsum of the mesosoma has concentric carinulae and sometimes is slightly punctate. The mesopleuron is smooth and shining except for punctuations and areolae on the ventral margin. The propodeal declivity is smooth with fine transverse striae. The petiole and postpetiole are dorso-laterally strigulate. The gaster is mostly smooth and shiny but sometimes finely and sparsely strigulate.

Distribution. The genus *Tatuidris* is restricted to the Neotropics, but it has an ample distribution that spans from northern Mexico to central Brazil, French Guiana (Lacau *et al.* 2012) and Amazonian Peru (Figure 13). No collections are known from the Caribbean, Galápagos, or other islands. Most specimens and collections are currently known to occur in localities west of the Andes, with more collections tending to occur towards Central America and Mexico. Most collections come from mountainside (pre-montane) areas at mid elevations (usually 800–1200m of altitude). Collections from lowland Amazonia are few.

Natural history. Little is known about the biology of the ant genus *Tatuidris* and, until recently, no observations of live specimens were registered. Details of a first collection event of a small live colony (3 workers and 4 gynes) by Dr. Thibaut Delsinne (pers. comm.) in a mid-elevation forest in southeastern Ecuador suggest that *Tatuidris* may well be a highly specialized predator, as colonies kept in captivity did not accept any food item offered to them. Food items rejected by the ants included live and dead termites, millipedes, mites, various insect parts, sugar water, tuna, biscuits, live and dead fruit flies (*Drosophila*), live springtails, live myriapods (Chilopoda and Diplopoda), live and dead Diplura, small live spiders, small live pseudoscorpions, one small snail, uncooked hen egg (i.e. piece of cotton wool soaked with fresh whisked hen egg; Brown 1977), ant larvae (*Gnamptogenys* sp.), and live ant workers (*Cyphomyrmex* sp., *Brachymyrmex* sp.). Potential food items (arthropods) for *Tatuidris* were taken from soil samples and Winkler samples (following Silva and Brandão 2010) collected at the site where *Tatuidris* was *a priori* determined to be present.
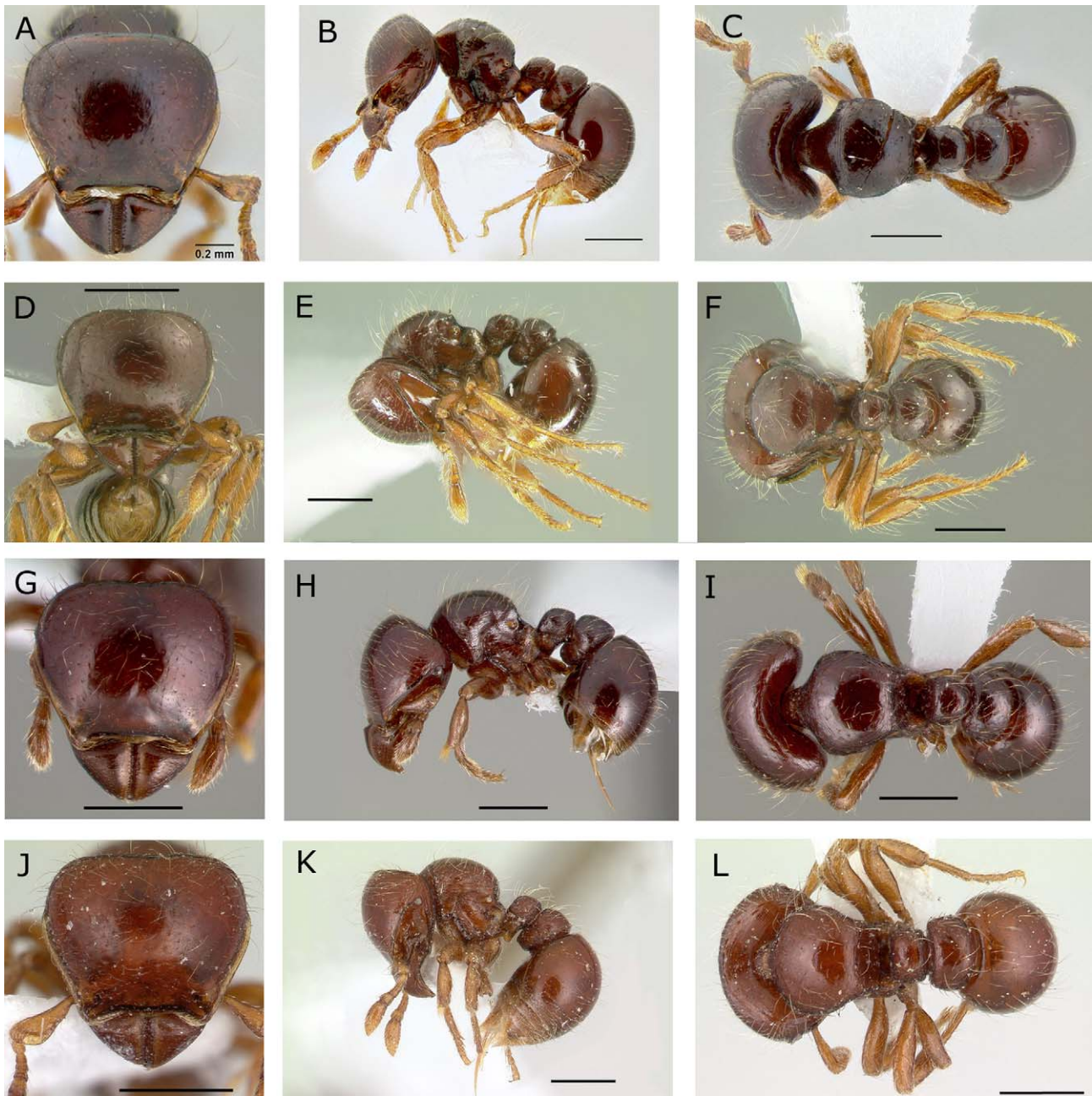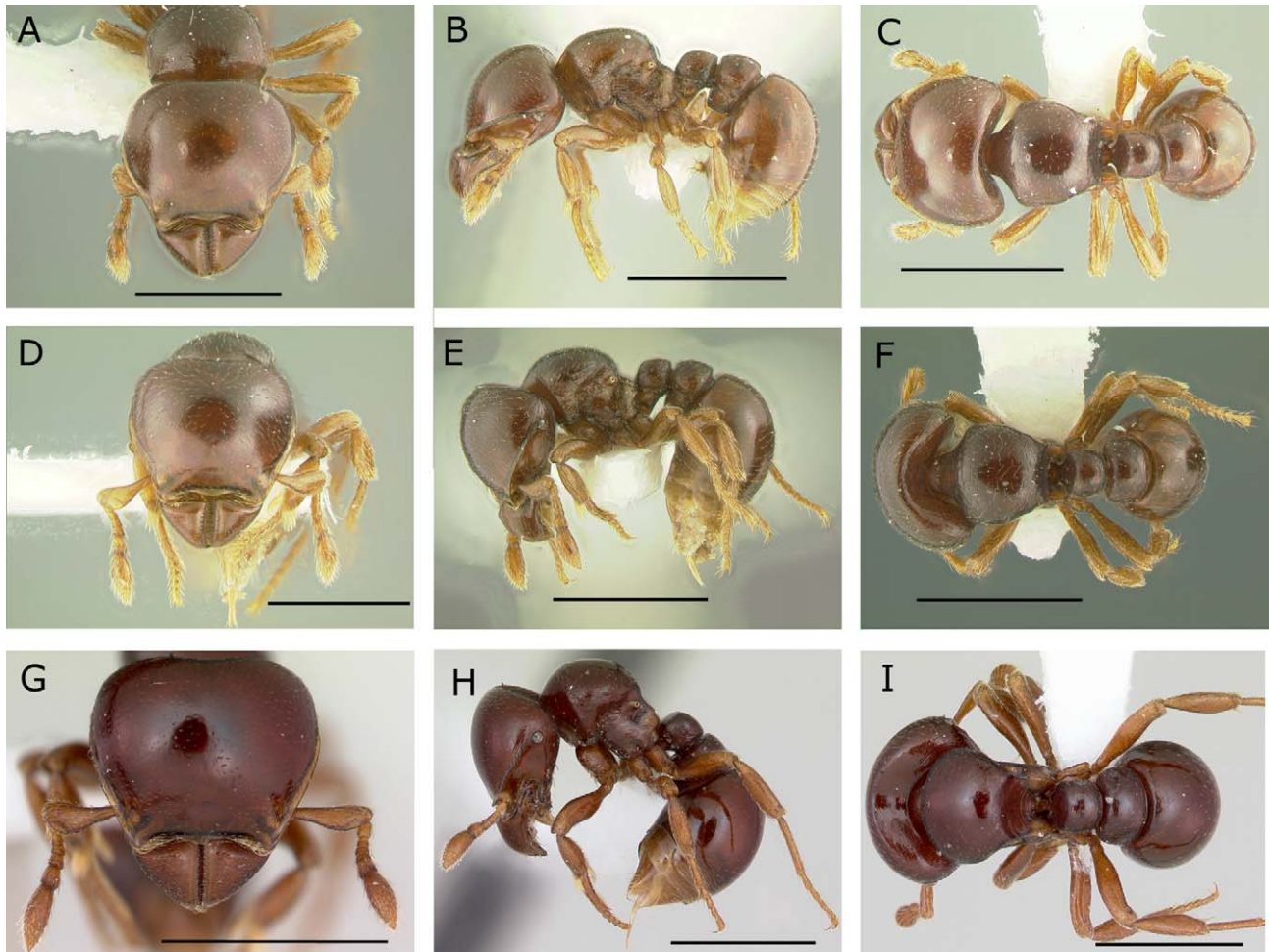
FIGURE 6. *Tatuidris tatusia* and specimens showing pilosity pattern A. A–C) Full face, lateral and dorsal view of *T. tatusia* from Matagalpa, Nicaragua; D–F) Full face, lateral and dorsal view of *T. tatusia* from Otongachi, Ecuador; G–I) Full face, lateral and dorsal view of *T. tatusia* from Maquipucuna, Ecuador; J–L) Full-face, lateral and dorsal view of *T. tatusia* from Cuzco, Peru. Images A–C and J–L courtesy of antweb.org.

Further observations by T. Delsinne suggest that *T. tatusia* may be a sit-and-wait predator, as "both workers and gynes moved very slowly and were very clumsy. They often remained motionless during several tens of seconds or even several minutes when disturbed (either by my handling or by the contact with another arthropod). It is difficult to see them as powerful predators!" (pers. comm.). These observations were mainly performed at night, suggesting that *T. tatusia* may be nocturnal, a hypothesis also supported by collection patterns. For example, in the Río Toachi forest of Ecuador *T. tatusia* specimens tend to fall in pitfall traps, instead of Winkler sacs (Donoso and Ramón 2009). Because pitfall traps usually work 24-h, but Winkler sacs generally uses litter sifted during the day, then ants with nocturnal habits may be underrepresented in Winkler samples. The small eyes of *Tatudris* species provide further support for this hypothesis.

Other. The relative position of eyes is highly variable within the species. For example, eye location ranges from being completely within the antennal scrobes to completely outside the scrobes (Figure 1b). In some cases

(specimen J.Longino#2088-S) the eye itself is located outside the antennal scrobe, but the eye's fossa is well marked and confluent with the antennal scrobe. In most specimens, the antennal carina bifurcates from the antennal scrobes and lies straight above the eyes. However, in specimens from Nicaragua (MGB#1179 colony collection), a strongly impressed antennal carina is present. In these specimens about 40% of the eye's area lies within the antennal scrobes. In the gyne, only ~1/6 of the eye lies within the antennal scrobes. A depression sometimes forms in the integument in the sides of the propodeum, below the propodeal spiracle and above the metapleural gland. The depth of this depression varies among specimens and tends to be deepest in larger specimens.

FIGURE 7. *Tatuidris tatusia* . Specimens showing pilosity pattern B. A–C) Full face, lateral and dorsal view of *T. tatusia* from Caves Branch, Belize; D–F) Full face, lateral and dorsal view of *T. tatusia* from Belmopan, Belize; G–I) Full-face, lateral and dorsal view of *T. tatusia* from Maquipucuna, Ecuador. Images G–I courtesy of antweb.org.

Justification for the synonymy. A comprehensive analysis of the description of *T. kapasi* suggests that the morphological characters proposed by Lacau and Groc (2012) to separate *T. kapasi* from *T. tatusia* lie within the continuous variability encountered in *Tatuidris* specimens across the Neotropics. Two considerations were taken. First, the description of *T. kapasi* relies on a relatively large specimen where sculpture, body profile and body proportions are expected to vary the most. Diagnostic characters of *T. kapasi* (i.e. occipital border more concave, clypeus with the free margin nearly straight and laterally concave, dorsum of mesosoma mostly sculptured with concentric rugulae and carinulae, and dorsum of the petiolar and postpetiolar nodes with superficial concentric rugulae and carinulae) are all present to some degree in larger specimens among the collections reviewed in the present study (Figures 6–9). Another diagnostic character of *T. kapasi* was denser pilosity without long setae (similar to Morph D), but setal patterns did not correlate with any morphology- or molecular-based grouping in this study. Second, the type locality of *T. kapasi* lies at a range limit of the genus, where morphological extremes might be expected.

Worker measurements (in mm) and indices: [average (min–max) of 10–58 specimens]: AScL 0.46 (0.31, 0.67); AScW 0.24 (0.18, 0.36); CIx 129.03 (117.07, 137.93); EL 0.05 (0.03, 0.08); FL 0.43 (0.31, 0.70); FW 0.11 (0.08,

0.17); HL 0.59 (0.43, 0.88); HW 0.76 (0.56, 1.10); IAD 0.36 (0.25, 0.54); PL 0.16 (0.10, 0.24); PpL 0.16 (0.10, 0.25); PW 0.25 (0.18, 0.37); PpW 0.36 (0.26, 0.53); PPpIx 68.92 (58.14, 80.00); PrW 0.52 (0.38, 0.77); TiL 0.35 (0.27, 0.52); TiW 0.10 (0.06, 0.17); WbL 0.62 (0.45, 0.89); SL 0.42 (0.32, 0.51); SW 0.13 (0.11, 0.17); SI 329.82 (300.00, 360.00); REL 9.02 (5.41, 11.48).
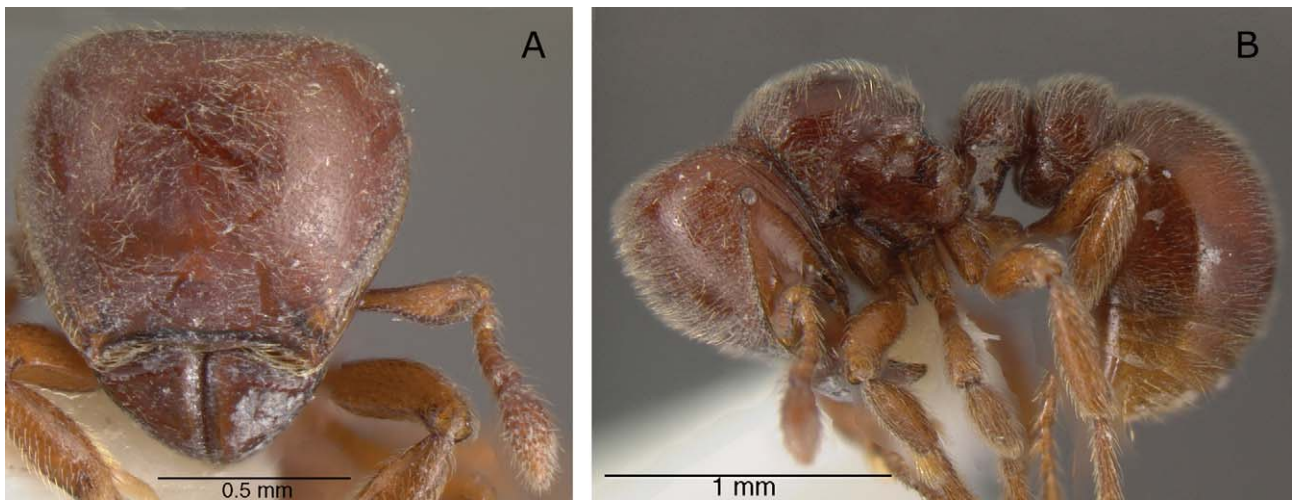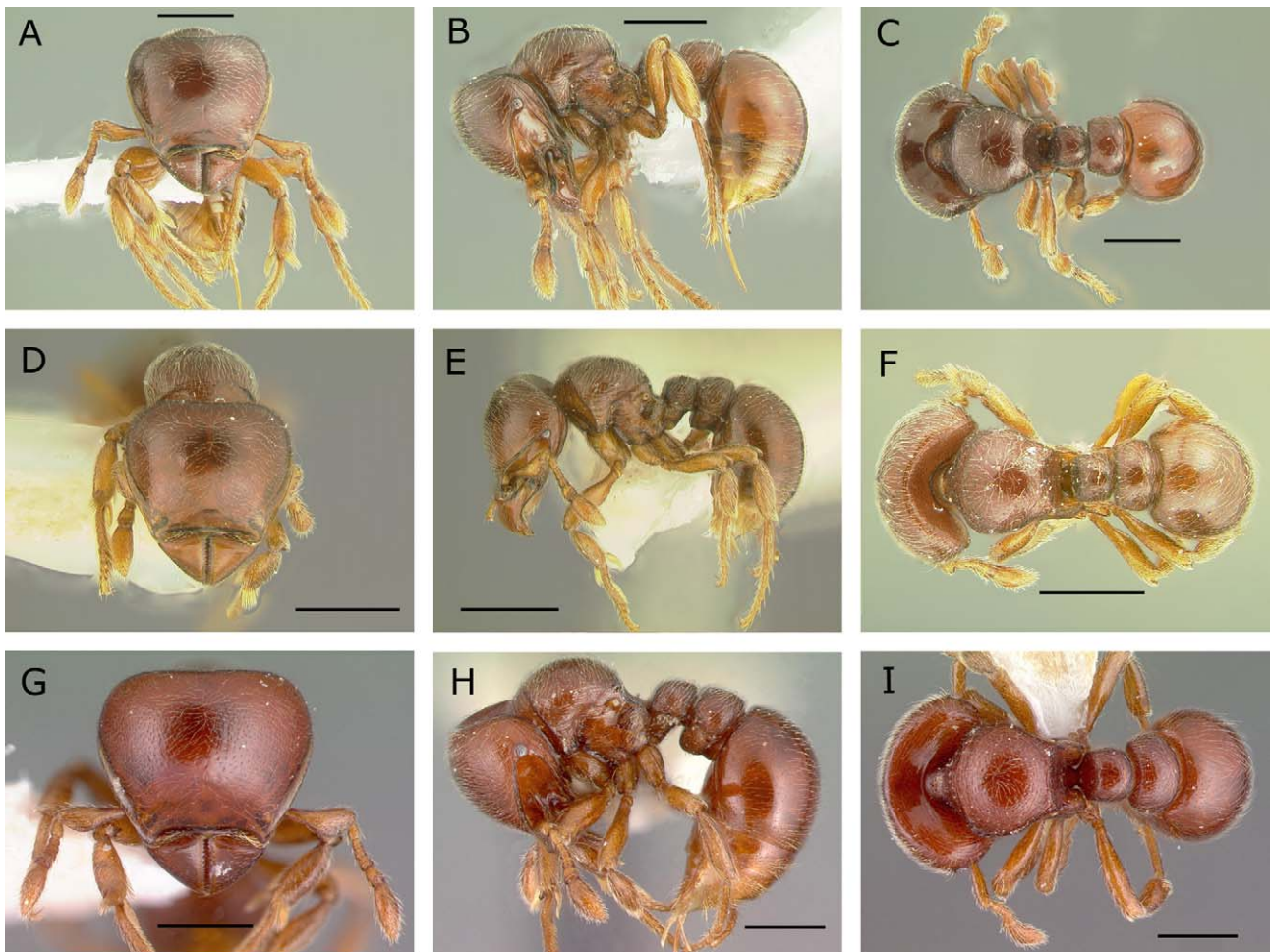

FIGURE 8. *Tatuidris tatusia* . Specimens showing pilosity pattern C. A) Full face and B) lateral view of *T. tatusia* from Puntarenas, Costa Rica.

FIGURE 9. *Tatuidris tatusia* . Specimens showing pilosity pattern D. A–C) Full face, lateral and dorsal view of *T. tatusia* from Los Tuxtlas, Mexico; D–F) Full face, lateral and dorsal view of *T. tatusia* from Chiapas, Mexico; G–I) Full face, lateral and dorsal view of *T. tatusia* from Magdalena, Colombia.
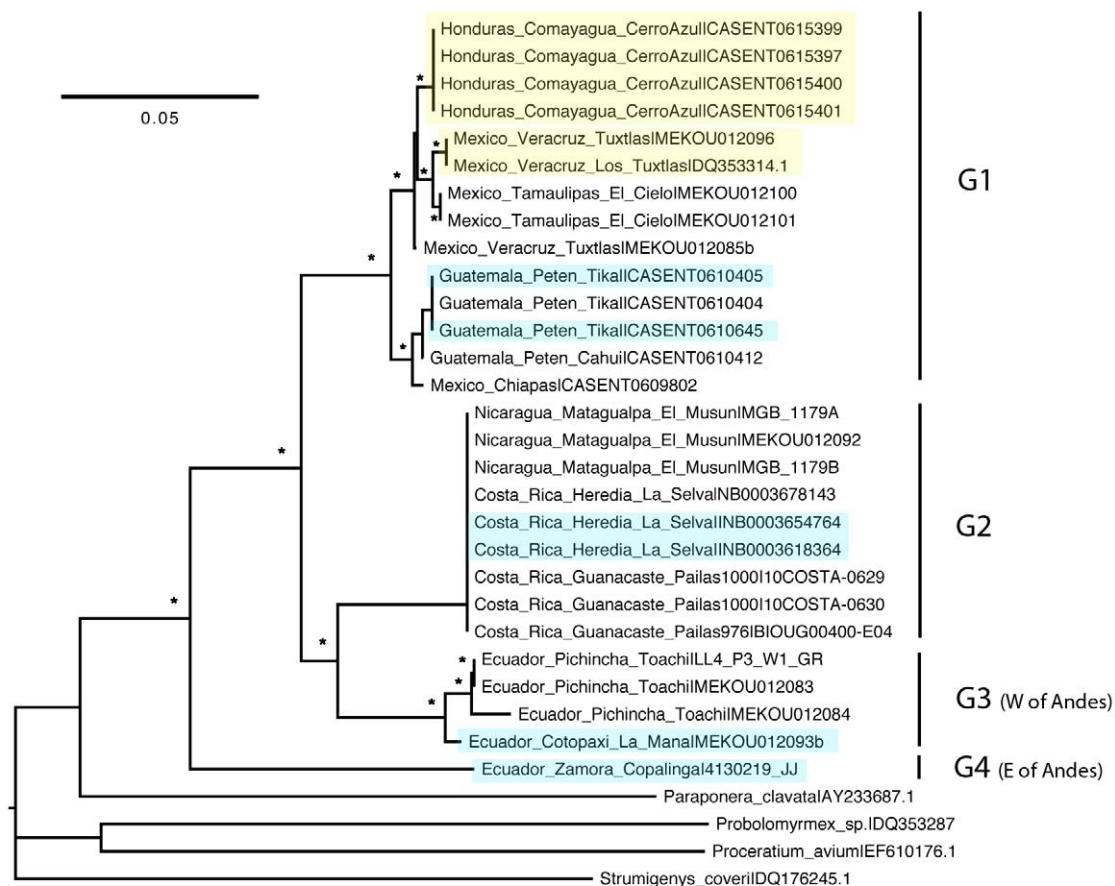
FIGURE 10. Neighbor joining tree based on K2P distances for 28 *Tatuidris* specimens and four other ant taxa (*Paraponera clavata*, *Probolomyrmex* sp., *Proceratium avium* and *Strumigenys coveri*) as outgroups. Labels consist of countries, first division, localities, and specimen IDs. Specimens with no color present a pilosity pattern "A", similar to the type series. Specimens with pilosity pattern "B" are highlighted in light blue. Specimens with pilosity pattern "D" are highlighted in yellow. No specimen with pilosity pattern "C" was available for sequencing. Asterisks above nodes represent nodes with >70% bootstrap support (999 repetitions). The tree is drawn to scale, with branch lengths in the same units as those of the genetic divergence inferred using the K2P model.

Gyne measurements (in mm) and indices: (n=1) AScL 0.47; AScW 0.15; EL 0.20; FFS 0.09; FL 0.77; FW 0.20; HL 0.88; HW 1.28; IAD 0.56; Pl 0.22; PPL 0.28; PPW 0.72; PW 0.45; TL 0.69; TW 0.20; WingL 4.60; WbL 1.53; REL 22.63.

Male measurements (in mm) and indices: (n=1) EL 0.32; FFS 0.13; HL 0.66; HW 0.88; IAD 0.21; ScL 0.11; WingL 3.6; WbL 1.22; FL 0.9; REL 48.44.

Specimens examined: Elements in this list follow this order: COUNTRY, *State or Province*, Locality, elevation, coordinates, collector (collection code, habitat, method) [specimen code], [REPOSITORY].

BELIZE, 2.5 millas S Belmopan, S&J Peck (B-242, Limestone forest, ex: Berlese) [MCZC]. Caves Branch, S&J Peck (B-248, Hi Canopi Forest, ex: Berlese [MCZC]. BRAZIL, *Amazonas*, Manaus, Universidade do Amazonas, 03°05'36"S; 59°57'52"W, E Pereira Franken (Terra Firme: PLATO, ex: Pitfall) [INPA]. COLOMBIA, *Magdalena*, El Campano, 1300m, 11°07'N; 74°06'W, Phillip Ward (#7891-9, montane rainforest, ex: Sifted litter, leaf mold, rotten log) [QCAZ]. COSTA RICA, Rincon de la Vieja, Pailas, 1000m, 10.7887, –85.349, A Smith (10COSTA-0629 and 10COSTA-0630, Primary Forest) [AlexSmith]. *Alajuela*, Casa Eladio, Rio Peñas Blancas, 800m, 10°19' N; 84°43' W, J Longino (Wet forest, ex: Sifted leaf litter) [INBIOCRI002280066, INBIOCRI002280068 and INBIOCRI002280065] [JTLC]. *Alajuela*, El Aleman, Rio Peñas Blancas, 6,5 Km E Monteverde, 940m, 10°18' N; 84°45' W, J Longino (#0861-s, Wet forest, ex: Sifted leaf litter) [INBIOCRI002280059] [JTLC]. *Heredia*, 16km SSE La Virgen, 1100m, 10°16'N; 84°05'W [INB0003214087, INB0003214014, INB0003214104, INB0003214131, INB0003214232 and INB0003212497] [INBC]. *Heredia*, La
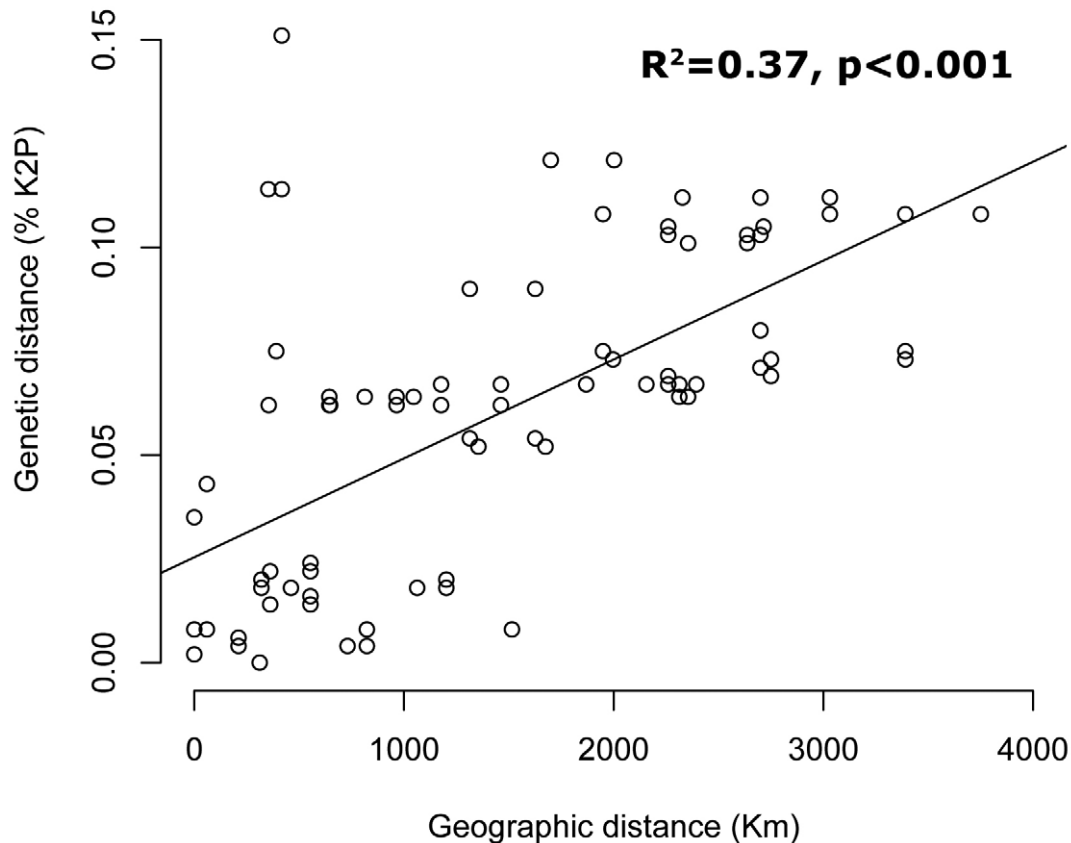
FIGURE 11. Linear regression between genetic distance (pairwise divergence) and geographic distance.

Selva Biological Station-1, 50m, M Molina and H Garcia (AMI-1-W-006-05) [JTLC]. *Heredia*, La Selva Biological Station-2, 50m, 10.433, –84.0167, J Longino (All ants from Louisa Stark (OTS 89-1 student) study, ex: Litter and ground-nesting) [INBIOCRI001281194 and INBIOCRI001281181] [JTLC]. *Heredia*, La Selva Biological Station-2, 09°09' N; 079°51' W, Michael Kaspari (45196.01 and 45000.6) [MEK]. *Puntarenas*, Rio San Luis, 850m, 10°17' N; 84°48' W, J. Longino (Moist forest, ex: Sifted leaf litter on ground) [INBIOCRI002280062 and INBIOCRI002280063] [JTLC]. ECUADOR, *Cotopaxi*, 19 km ENE La Maná, 1100m, 00°53' S; 79°03' W, Phillip Ward (#11418-6, Second-Grown Rainforest, ex: Sifted leaf litter and logs) [QCAZ]. *Pichincha*, R.B. Maquipucuna, 1200m, 00°07'00"N; 78°38'06W, R Anderson (#99-208-6 and #99-208, Montane evergreen forest) [CASENT0423526 and CASENT0001968] [CASC]. *Pichincha*, Unión del Toachi-Otongachi, 850m, 00°21'05"S; 78°57'10"W, Donoso & Vieira (Bosque Secundario, ex: Pitfall) [18 workers and 1 gyne, MEKOU12079-84 and MEKOU12103-4] [QCAZ]. *Zamora*, Bombuscaro Numex, 950m, –4.114972 S; –78.96794 W, M Leponce (SPM_33796, Evergreen premontane rainforest, ex: Winkler sample) [QCAZ]. *Zamora*, Copalinga Private Reserve, 1000m, –4.0912222 S; –78.96069 W, T Delsinne and T. Arias-Penna (SPM_4130219, Secondary evergreen premontane rainforest, ex: Winkler sample) [QCAZ]. EL SALVADOR [Paratype and Holotype], 2 mi. S Quetzaltepec, ME Erwin [MCZ Paratype 31577] [MCZC]. GUATEMALA, *Peten*, Parq. Nac. Tikal, 270m, 17.232 N; –89.623 W (Tropical Moist Forest) [CASC]. HONDURAS, *Comayagua*, PN Cerro Azul Meambar, 1120m, 14.887136; –87.89974 (LLAMA#Wa-C-04-1-15, Ridgetop cloud forest, ex: Sifted leaf litter) [CASENT 0615399] [CASC]. MEXICO, *Chiapas*, 860m, 16.980 N; –91.586 W, MG Branstetter (#856, Mesophil forest) [QCAZ]. *Chiapas*, 12 mi NW Ocozocoautla, 400m, A Newton (ex: Berlese) [MCZC]. *Chiapas*, 6kmSW Ocosingo, 1400m, 16.867221 N; –92.0787132 W, R Anderson (# 91–116, Forest litter, ex: Berlese) [CASENT 0603397] [INBC]. *Chiapas*, Lago Metzabok, 575m, 17.124, –91.636, MG Branstetter (Lowland wet forest) [CASC]. *Oaxaca*, Mirador Grande, 990m, 17.89844, –96.36253, MG Branstetter (#1405) [QCAZ]. *Tamaulipas*, El Cielo, 870m, 23.276, –99.276, MG Branstetter (#1465) [QCAZ]. *Veracruz*, Los Tuxtlas, Ejido-López Mateos, 50m, 18°24'56"N; 94°56'53"W, P Rojas (LM7S-H1, LM42S-H4, LM42S-H5 and LM21A-H3, Selva alta perennifolia, ex: Winkler) [IEXM]. *Veracruz*, Los Tuxtlas, Ejido-López Mateos, Ejido 2, 50m, 18°24'56"N; 94°56'53"W, P Rojas (LM42S-

H3, Selva alta perennifolia, ex: Winkler) [IEXM]. *Veracruz*, Los Tuxtlas, Volcán S. M. Pajapan, 510m, 18°16'00"N; 94°46'71"W, A Cartas (847d, Selva mediana subperennifolia, ex: Berlese) [IEXM]. NICARAGUA, *Matagalpa*, RN El Musún, 4.8km NNW Rio Blanco, 1170m, 12°58.4'N; 085°14'W, M.G.Branstetter (#1179, Mesic forest, ex: Sifted leaf litter) [QCAZ]. PANAMA, *Chiriqui*, 20,4 Km North San Felix, R. Anderson (#17768_1, Wet mountain forest, ex: Litter sample) [WEMC]. *Chiriqui*, Alto Lino, 3800m, HG Real [Male, CASENT 0102681] [CASC]. *Chiriqui*, La Fortuna, Finca La Suisse, 1200m, R. Anderson (#17838, #17787, #17788, #17789, #17790, #17838 and #17839 [WEMC]. PERU, *Cuzco*, La convención Province, 4 km S Camisea River. Campamento Cashiriari-2, Plot 1, 579m, 11°51'51.3"S; 72°46'45.6"W, J Santisteban et al. (#38, Primary Rainforest, hilly terrain, ex: Winkler Trap) [MUSM-ENT 0201599/ANTWEB-CASENT 0178882] [MUSM].
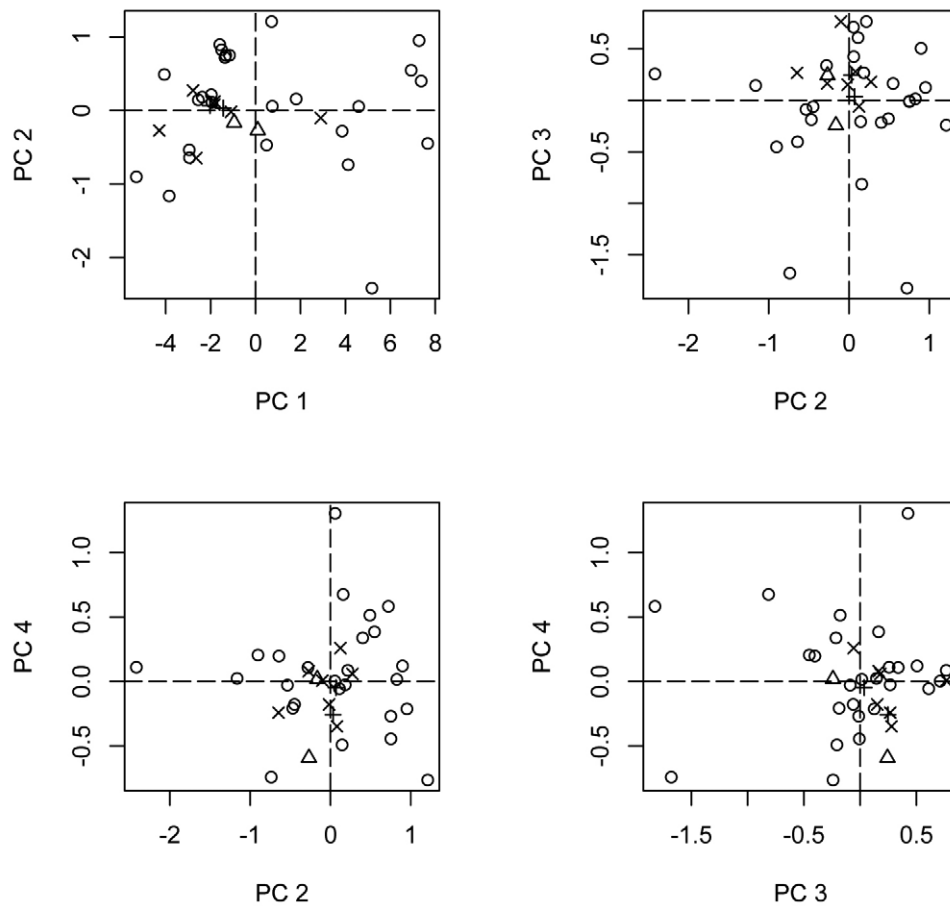

FIGURE 12. PC scores for specimens included in this analysis. Symbols represent different pilosity patterns. Circles = pilosity pattern A (similar to type series). Crosses = pilosity pattern B. Triangles = pilosity pattern C. X's = pilosity pattern D.

Discussion

More than 40 years after the original description by Brown and Kempf (1968), *Tatuidris* remains a remarkable and rather unknown ant genus. Here I hypothesize that all specimens reviewed comprise one species, *Tatuidris tatusia*. I base this hypothesis on analysis of variability of morphological and barcode data. The morphological analysis presented here suggests that most size variability encountered among specimens is continuous, a fact that will likely continue hindering species delimitations. I also described differences in pilosity and pubescence patterns I have encountered within collections. While this approach is not unique within ants and pilosity patterns have been used to delimit species in ant genera like *Myrmecocystus* (Snelling 1976), *Formica* (Francoeur 1973), *Rogeria* (Kugler 1994) and *Linepithema* (Wild 2008), I conclude that pilosity patterns do not offer good species-level differentiation for *T. tatusia*. Other meristic and continuous characters between the material examined are extremely uniform (e.g. body size, shape), or too variable (e.g. color, and sculpturing) and currently do not offer a

clear separation of specimens into species. Nonetheless, I am aware that the addition of new data (e.g. molecular, behavioral, internal anatomy, etc.), better analytic methods or new collections of gynes and males may improve the species delimitation I propose in this work.
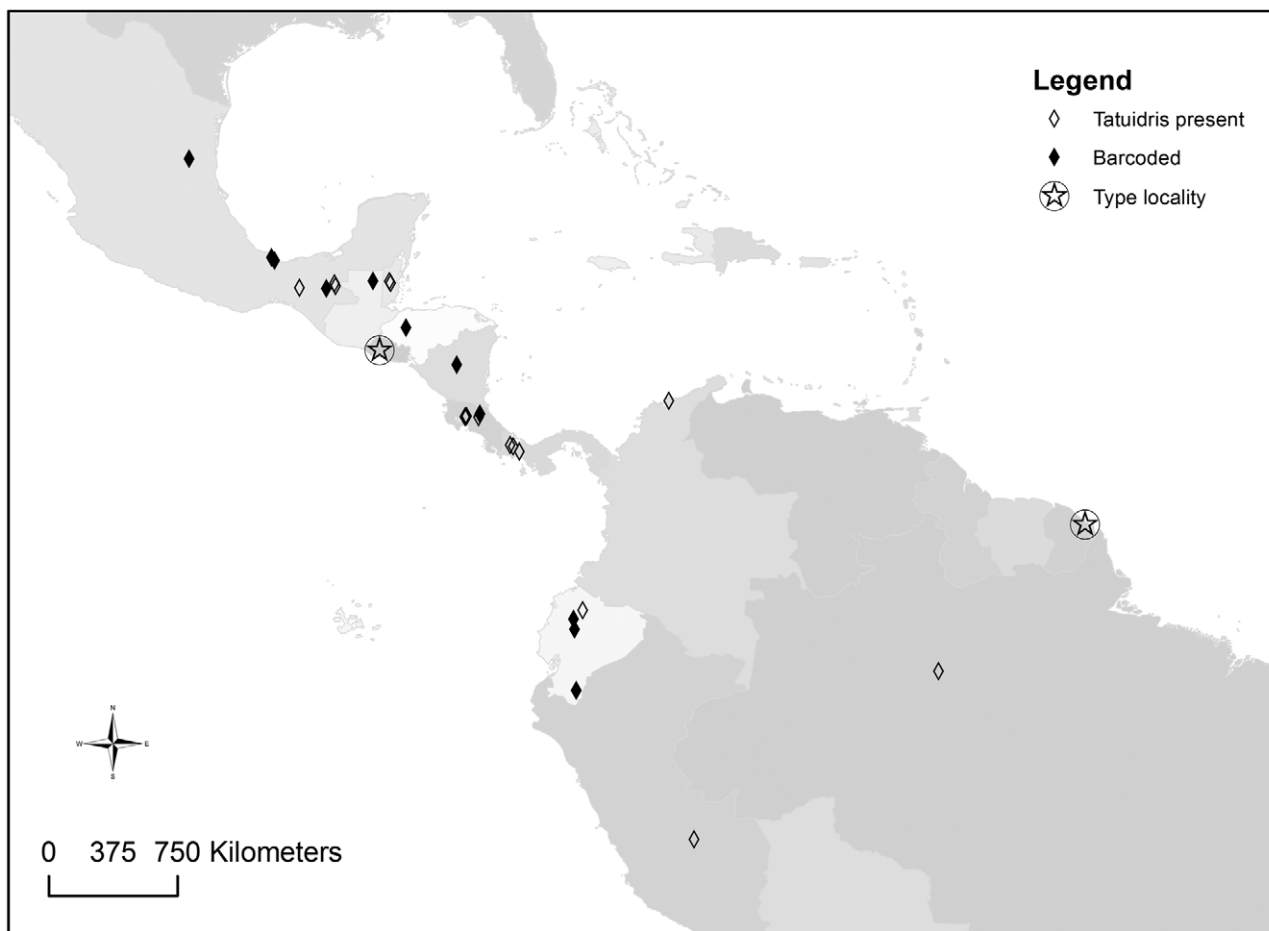

FIGURE 13. Map of localities of specimens included in this study. Black diamonds represent localities from which specimens included in the CO1 DNA barcodes analysis were obtained. Circled stars represent type localities from the two previously know species (e.g. *Tatuidris tatusia* Brown and Kempf, and *Tatuidris kapasi* Lacau and Groc **syn. nov.**).

Molecular analysis based on DNA barcodes presented a pattern more difficult to explain. The intraspecific variability among individuals was 7 times larger than usually encountered among species (i.e. 2%, Ratnasingham and Hebert 2007, Smith and Fisher 2009, Jansen *et al.* 2009), which suggests that *Tatuidris* represents a single lineage undergoing genetic isolation by distance, a pattern consistent with allopatric differentiation. Alternatively, DNA barcode results suggest that several cryptic species remain to be described. Within ants, analysis of DNA barcode data has proved a valid tool to delimit species (Smith *et al.* 2005, Fisher and Smith 2008), although this has not always been the case (Jansen *et al.* 2009, Wild 2009) and species delimitations always benefit from analysis of additional genes [e.g. wingless (WG), Elongation Factor 1-α (EF1-α), long-wavelength rhodopsin (LWR) and internal transcribed spacer (ITS-1 and ITS-2); Fisher and Smith 2008, Wild 2009, Nieukerken *et al.* 2012]. While the level of CO1 variability observed in this study could justify four species with strong geographic segregation (i.e., barcode clusters G1–G4, Figure 10), I conservatively avoided doing so because no clear morphological separation among DNA barcode groups is recovered from either a) the PCA analysis, or b) the distribution of pilosity patterns in the NJ tree. Naming species that are recognizably only by molecular techniques will likely result in taxonomic confusion.

The phylogenetic position of *Tatuidris* within Formicidae remains a challenging work. For example, a recent revision of the poneromorphs by Keller (2011) provides new evidence for a rearrangement of internal phylogeny of Formicidae that differ from both molecular and traditional morphological approaches. One morphological

autapomorphy for *Tatuidris* described by Keller (2011) was the position of the antennal socket, which, in this genus, sits upside-down on the roof of the frontal lobe. Such position of the antennal sockets is easily recognizable when ants are viewed with head in full-face view as small "blisters". A closer examination of this character among other ant genera suggests that *Phalacromyrmex*, an ant genus traditionally associated with *Tatuidris*, may present this character as well (Figure 14). Here I hypothesize that further re-examination of this character as well as analysis of molecular characters of *Phalacromyrmex* will likely shed light on the origin and phylogenetic status of *Tatuidris*.

FIGURE 14. Lateral-diagonal view of head of *Phalacromyrmex* sp., from Brazil, showing position of antennal sockets on head capsule. In *Phalacromyrmex*, the antennal socket is located up-side down in a way similar to that of *Tatuidris*. Photo courtesy of R. Feitosa.

Acknowledgements

anonymous reviewers. Laboratory analyses on sequences generated at the Biodiversity Institute of Ontario were funded by the Government of Canada through Genome Canada and the Ontario Genomics Institute (2008-0GI-ICI-03). This work was submitted in partial fulfillment of the author's PhD degree at the University of Oklahoma. Mike Kaspari, May Yuan, Yiqi Luo, Laurie Vitt and Rich Broughton served on the author's doctoral committee and provided valuable guidance throughout the program.

Literature Cited

Baroni Urbani, C. & De Andrade, M.L. (2007) The ant tribe Dacetini: Limits and constituent genera, with descriptions of new species. *Annali del Museo Civico di Storia Naturale "G. Doria"*, 99, 1–191.
Bolton, B. (1984) Diagnosis and relationships of the myrmicine ant genus *Ishakidris* gen. n. (Hymenoptera: Formicidae). *Systematic Entomology*, 9, 373–382.
Bolton, B. (2003) Synopsis and classification of Formicidae. *Memoirs of the American Entomological Institution*, 71, 1–370.
Brady, S.G., Schultz, T.R., Fisher, B.L. & Ward, P.S. (2006) Evaluating alternative hypotheses for the early evolution and diversification of ants. *Proceedings of the National Academy of Sciences, USA*, 103, 18172–18177.
Brown, W.L. (1977) An aberrant new genus of myrmicine ant from Madagascar. *Psyche*, 84, 218–224.
Brown, W.L. (1979) A Remarkable New Species of Proceratium, With Dietary and Other Notes on the Genus (Hymenoptera: Formicidae)," *Psyche*, 86, 337-346.
Brown, W.L. & Kempf, W.W. (1968) *Tatuidris*, a remarkable new genus of Formicidae (Hymenoptera). *Psyche*, 74, 183–190.
Carpenter, F.M. (1930) The fossil ants of North America. *Bulletin of the Museum of Comparative Zoology*, 70, 1–66.
Carpenter, F.M. (1935) A new name for *Lithomyrmex* Carp. (Hymenotera). *Psyche*, 42, 91.
Felsenstein, J. (1985) Confidence limits on phylogenies: An approach using the bootstrap. *Evolution*, 39, 783–791.
Fernández, F. (2002) New ants records for Colombia and South America (Hymenoptera: Formicidae). *Revista Colombiana de Entomología*, 28, 215.
Fisher, B.L. and Smith, M.A. (2008) A revision of malagasy species of *Anochetus* Mayr and *Odontomachus* Latreille (Hymenoptera: Formicidae). *PLoS ONE*, 3, e1787.
Francoeur, A. 1973. Révision taxonomique des espèces néarctiques du groupe fusca, genre Formica (Formicidae, Hymenoptera). *Memoires de la Sociéte Entomologique du Quebec*, 3, 1–316.
Hebert, P.D.N., Cywinska, A, Ball, S.L. & Dewaard, J.R. (2003) Biological identifications through DNA barcodes. *Proceedings of the Royal Society of London Series B, Biological Sciences*, 270, 313–321.
Jansen, G., Savolainen, R. & Vepsalainen, K. (2009) DNA barcoding as a heuristic tool for classifying undescribed Nearctic *Myrmica* ants (Hymenoptera: Formicidae). *Zoologica Scripta*, 38, 527–536.
Keller, R.A. (2011) A phylogenetic analysis of ant morphology (Hymenoptera: Formicidae) with special reference to the poneromorph subfamilies. *Bulletin of the American Museum of Natural History*, 355, 1–90.
Kimura, M. (1980) A simple method for estimating evolutionary rate of base substitutions through comparative studies of nucleotide sequences. *Journal of Molecular Evolution*, 16, 111–120.
Kugler, C. (1994) A revision of the ant genus Rogeria with description of the sting apparatus (Hymenoptera: Formicidae). *Journal of Hymenoptera Research*, 3, 17–89.
Lacau, S, Groc, S., Dejean, A. de Oliveira, M.L. & Delabie J.C.H. (2012) *Tatuidris kapasi* sp. nov.: a new armadillo ant from French Guiana (Formicidae: Agroecomyrmecinae). *Psyche*, 2012, Article ID 926089, 6 pages, doi:10.1155/2012/926089
Longino J.T., Coddington, J. & Colwell, R.K. (2002) The ant fauna of a tropical rain forest: estimating species richness three different ways. *Ecology*, 83, 689–702.
Moreau, C.S. & Bell, C.D. (2011) Fossil Cross-validation of the dated ant phylogeny (Hymenoptera: Formicidae). *Entomologica Americana*, 117, 127–133.
Moreau, C.S., Bell, C.D., Vila, R., Archibald, S.B. & Pierce, N.E. (2006) Phylogeny of the ants: diversification in the age of angiosperms. *Science*, 312, 101–104.
Nieukerken, E.J. van, Doorenweerd, C., Stokvis, F.R. & Groenenberg, D.S.J. (2012) DNA barcoding of the leaf-mining moth subgenus *Ectoedemia* s. str. (Lepidoptera: Nepticulidae) with CO1 and EF1-α: two are better than one in recognizing cryptic species. *Contributions to Zoology*, 81, 1–2.
Rabeling, C. Brown, J.M. & Verhaagh, M. (2008) Newly discovered sister lineage sheds light on early ant evolution. *Proceedings of the National Academy of Sciences, USA*, 105, 14913–14917.
Ratnasingham, S. & Hebert, P.D.N. (2007) BOLD: The Barcode of Life Data System (www.barcodinglife.org). *Molecular Ecology Notes*, 7, 355–364.
Rojas, P. (1996) Formicidae (Hymenoptera). *In*: Llorente, J., García-Aldarte, A. and González-Soriano E. (Eds.). *Biodiversidad, taxonomía y biogeografía de artrópodos de México: hacia una síntesis de su conocimiento*. IBUNAM, México D. F., pp. 483–500.
Saitou, N. & Nei, M. (1987) The neighbor-joining method: A new method for reconstructing phylogenetic trees. *Molecular Biology and Evolution*, 4, 406–425.
Serna, F., Bolton, B. & Mackay, W. (2011) On the morphology of *Procryptocerus* (Hymenoptera: Formicidae). Some

DONOSO

comments and corrigenda. *Zootaxa*, 2923, 67–68

Silva, R.R. & Brandão, C.R.F. (2010) Morphological patterns and community organization in leaf-litter ant assemblages. *Ecological Monographs*, 80, 107–124

Smith, M.A., Fisher, B.L. & Hebert, P.D.N. (2005) DNA barcoding for effective biodiversity assessment of a hyperdiverse arthropod group: the ants of Madagascar. *Philosophical transactions of the Royal Society of London. Series B, Biological Sciences*, 360, 1825–1834.

Smith, M.A. & Fisher, B.L. (2009) Invasions, DNA barcodes, and rapid biodiversity assessment using ants of Mauritius. *Frontiers in Zoology*, 6, 31.

Snelling, R.R. (1976) A revision of the honey ants, genus *Myrmecocystus* (Hymenoptera: Formicidae). *Natural History Museum of Los Angeles County Science Bulletin*, 24, 1–163.

Tamura, K., Dudley, J., Nei, M., and Kumar, S. (2007) MEGA4: Molecular Evolutionary Genetics Analysis (MEGA) software version 4.0. *Molecular Biology and Evolution*, 24, 1596–1599.

Vasconcelos, H.L. & Vilhena, J.M. (2003) First record of the ant genus *Tatuidris* (Hymenoptera: Formicidae) in Brazil. *In*: Alvarez-León, Ricardo. Ampliaciones de ambito. *Revista de Biología Tropical*, 51, 261–284.

Vieira, J.M. (2004) Confirmación de la presencia de *Tatuidris* Brown & Kempf, 1968 (Hymenoptera: Formicidae: Agroecomyrmecinae) en Ecuador. *Boletín de la Sociedad Entomológica Aragonesa*, 35, 294.

Ward, P.S. (2009) Taxonomy, phylogenetics, and evolution. Pp. 3–17 in: Lach, L., Parr, C. L., Abbott, K. (eds) *Ant ecology*. Oxford, Oxford University Press, 410 pp

Ward, P.S. (2011) Integrating molecular phylogenetic results into ant taxonomy (Hymenoptera: Formicidae). *Myrmecological News*, 15, 21–29.

Wheeler, W.M. (1914) The ants of the Baltic amber. *Schriften derphysikaliscli-oekononiis-chen Gesellschaft zu Konigsberg*, 55, 1–142.

Wheeler, G.C. & Wheeler, J. (1976) Ant larvae: review and synthesis. *Memoirs of the Entomological Society of Washington*, 74, 1–108.

Wild, A.L. (2009) Evolution of the Neotropical ant genus *Linepithema*. *Systematic Entomology*, 34, 49–62.

Yoshimura, M. & Fisher, B.L. (2007) A revision of male ants of the Malagasy region (Hymenoptera: Formicidae): Key to subfamilies and treatment of the genera of Ponerinae. *Zootaxa*, 1654, 21–40

Yoshimura, M. & Fisher, B.L. (2009) A revision of male ants of the Malagasy region (Hymenoptera: Formicidae): Key to genera of the subfamily Proceratiinae. *Zootaxa*, 2216, 1–21.